Relativistic Electron Microbursts as High Energy Tail of Pulsating Aurora Electrons

Y. Miyoshi[1], S. Saito[2], S. Kurita[3], K. Asamura[4], K. Hosokawa[5], T. Sakanoi[6], T. Mitani[4], Y. Ogawa[7], S. Oyama[1,7] , F. Tsuchiya[6], S. L. Jones[8], A. N. Jaynes[9], and J. B. Blake[10]

[1]Institute for Space-Earth Environmental Research Nagoya University, Nagoya, Japan
[2]National Institute of Information and Communications Technology, Koganei, Japan
[3]Research Institute for Sustainable Humanosphere, Kyoto University, Uji, Japan
[4]Institute of Space and Astronautical Science, Japan Aerospace Exploration Agency, Sagamihara, Japan
[5]The University of Electro-Communications, Chofu, Japan
[6]Graduate School of Science, Tohoku University, Sendai, Japan
[7]National Institute of Polar Research, Tachikawa, Japan
[8]Goddard Space Flight Center, NASA, Greenbelt, MD, US
[9]Department of Physics and Astronomy, University of Iowa, Iowa City, IA, US
[10]Aerospace Corporation, Los Angeles, CA, US.

Corresponding author: Y. Miyoshi (miyoshi @ isee.nagoya-u.ac.jp)

Key Points:

- We demonstrate that sub-relativistic/relativistic electron microbursts are the high-energy tail of pulsating aurora electrons.
- Our simulation studies demonstrate that both pulsating aurora and relativistic electron microbursts originate simultaneously.
- Pulsating aurora electron and relativistic electron microbursts are the same product of chorus wave-particle interactions,

Abstract

In this study, by simulating the wave-particle interactions, we show that sub-relativistic/relativistic electron microbursts form the high-energy tail of pulsating aurora (PsA). Whistler-mode chorus waves that propagate along the magnetic field lines at high latitudes cause precipitation bursts of electrons with a wide energy range from a few keV (PsA) to several MeV (relativistic microbursts). The rising tone elements of chorus waves cause individual microbursts of sub-relativistic/relativistic electrons and the internal modulation of PsA with a frequency of a few Hz. The chorus bursts for a few seconds cause the microburst trains of sub-relativistic/relativistic electrons and the main pulsations of PsA. Our simulation studies demonstrate that both PsA and relativistic electron microbursts originate simultaneously from pitch angle scattering by chorus wave-particle interactions.

Plain Language Summary

Pulsating aurora electron and relativistic electron microbursts are precipitation bursts of electrons from the magnetosphere to the thermosphere and the mesosphere with energies ranging from a few keV to tens of keV, and sub-relativistic/relativistic, respectively. Our computer simulation shows that pulsating aurora electron (low energy) and relativistic electron microbursts (high energy) are the same product of chorus wave-particle interactions, and relativistic electron microbursts are high-energy tail of pulsating aurora electrons. The relativistic electron microbursts contribute to significant loss of the outer belt electrons, and our results suggest that the pulsating aurora activity is a proxy of the radiation belt flux variations.

1 Introduction

[1]
Pulsating auroras (PsA) are caused by the intermittent precipitation of electrons with energies ranging from a few keV to ~100 keV from the magnetosphere to the upper atmosphere (e.g., Sandahl, 1980; Miyoshi et al., 2010). Lower-band chorus (LBC) waves cause the precipitation of these electrons through pitch angle scattering (e.g., Miyoshi et al., 2010; Nishimura et al., 2010; 2020; Jones et al., 2009; Lessard, 2012; Jaynes et al., 2013; Kasahara et al., 2018). Miyoshi et al. (2015a) have proposed a model to describe the relationship between the energy spectrum of the precipitating electrons in PsA and the frequency spectrum of LBC. The intermittent precipitations of energetic electrons occurring every few seconds, which are responsible for the main modulations of the PsA, are caused by the LBC bursts. The internal modulations with a frequency of a few Hz are caused by rising tone elements of LBC embedded in each LBC burst. This model has been confirmed by recent conjugate observations (Kasahara et al., 2018; Ozaki et al., 2019; Hosokawa et al., 2020) by the Arase satellite (Miyoshi et al., 2018) and ground-based instruments. Miyoshi et al.(2015a) have also shown that stable precipitations from multi-hundred eV to ~ a few keV are caused by the upper-band chorus (UBC) waves.

[2]
Relativistic electron microbursts are a short-lived burst of precipitation of electrons having energies ranging from a few hundred keV to MeV (Imhof et al., 1992; Nakamura et al., 1995; Blake et al., 1996, Tsurutani et al., 2013, Blum and Breneman, 2020). The typical spatial scale of

these microbursts is on the order of tens of kilometers (Shmuko et al., 2018). The duration of the individual bursts is ~100 ms, which belongs to the same time scale as the internal modulations of the PsA and the rising tone of LBC. Anderson and Milton (1964) first reported aurora microbursts based on X-ray observations and showed that the microbursts tend to occur in "trains", where a series of 3 to 15 microbursts occur in a periodic sequence that typically would span several seconds. Recent observations have shown that these microbursts are caused by the pitch angle scattering from chorus waves (Brenemann et al., 2017; Shumko et al., 2020).

[3]

Figure 1(a) shows typical pulsating aurora electrons of 8 keV from the low-altitude Reimei satellite (Asamura et al., 2004). The optical camera onboard the Reimei satellite (Sakanoi et al., 2004) detected PsA along the footprint of the satellite. The main modulations and the internal modulations are seen in the precipitating electrons. **Figure 1(b)** shows >30 keV electrons measured by LEICA (Mason et al., 1993), >450 keV electrons measured by PET (Cook et al., 1993) and >1 MeV electrons measured by HILT (Klecker et al., 1996) of Solar, Anomalous, and Magnetospheric Particle Explorer (SAMPEX) . The time resolutions of the data are 1 sec (b) , 50 msec (c) and 20 msec (d), respectively. The precipitations of each energy range are concurrently observed. At **Figure 1 (c) (d)**, the individual microbursts are clearly seen. Along with the individual microbursts, the trains, each of which is a series of several bursts, are seen in this observation.

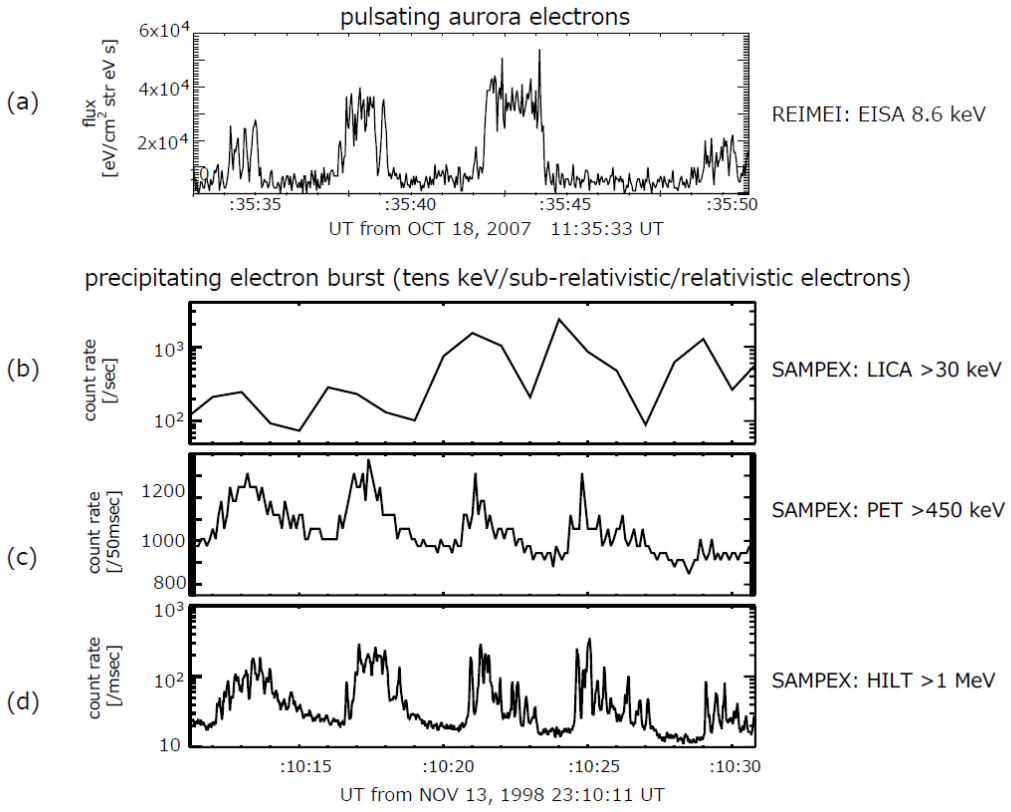

Figure 1. Variation of the precipitating electron flux with respect to time at an altitude of ~100 km. (a) Typical variations of the precipitating electrons associated with the pulsating aurora

116 measured by Reimei. The corresponding energy is 8.7 keV. (b) Typical variations of
117 precipitating electrons of > 30 keV, (c) >450 keV and (d) >1 MeV measured by SAMPEX. The
118 time resolution of each data are 1 sec (b), 50 msec (c) and 20 msec (d), respectively.
119
120 [4]
121 Although the relationship between PsA and microbursts has not been clearly understood, they are
122 believed to originate from electron scattering by LBC. Sandahl et al. (1980) showed that ~140
123 keV electrons simultaneously precipitate into the ionosphere during PsA by a sounding rocket
124 experiment. Jones et al. (2009) showed enhanced ionization at altitudes <100 km using PFISR
125 observations during PsA. Miyoshi et al.(2015b) and Oyama et al.(2017) have shown, by using
126 the EISCAT radar observations, that sub-relativistic and relativistic electrons precipitate into the
127 atmosphere at altitudes <70 km in association with PsA. The microbursts of relativistic electrons
128 are also observed above the diffuse aurora (Kurita et al., 2015). These observations suggest that
129 sub-relativistic/relativistic electron microbursts often occur simultaneously with PsA and diffuse
130 aurora. Moreover, we expect that microburst trains are related to sub-second modulations
131 embedded within the main pulsation of PsA, because both variations have the same time scales.
132
133 [5]
134 When LBC propagate to high latitudes along the field lines, the resonance energy of the chorus
135 waves becomes high because of variations of the wave dispersion relation (Horne and Thorne,
136 2003). Miyoshi et al. (2010; 2015b) have proposed a model for wide energy precipitation of
137 electrons having energies ranging from a few keV to several MeV by LBC propagating along the
138 field line. Saito et al. (2012) have shown the possible energy dispersion curve for precipitating
139 electrons by considering relativistic effects using a test-particle computer simulation.
140
141 [6]
142 Considering these previous studies on PsA and microbursts, we propose a hypothesis that PsA
143 and microburst originate simultaneously from the LBC wave-particle interactions, when LBC
144 propagates to high latitudes along the field line. To confirm this hypothesis, we conducted a
145 computer simulation for the wave-particle interactions and the resultant precipitation of wide
146 energy electrons. We investigated the full-energy spectrum of the precipitating electrons for the
147 first time associated with the chorus wave-particle interactions.
148

149 **2 Simulations**

150
151 [7]
152 We used the geospace environment modeling system for integrated studies-radiation belt with
153 wave-particle interaction module (GEMSIS-RBW) test particle simulation (Saito et al., 2012),
154 which simulates the wave-particle interaction process between LBC propagating along the field
155 line and the bouncing electrons. The simulation estimates the temporal variation of the energy of
156 the precipitating electrons at an altitude of 100 km. The momentum changes associated with the
157 wave-particle interaction are given by the following equation of motion:
158 $$\frac{d}{dt}\mathbf{p_e} = q\left(\delta\mathbf{E} + \mathbf{v_e}\times\left(\mathbf{B}+\boldsymbol{\delta}\mathbf{B}\right)\right),$$

where $\mathbf{v_e} = \mathbf{p_e} / m_e\gamma$ is the electron velocity, $\mathbf{B}$ is the background magnetic field vector, $\mathbf{p_e}$ is the electron momentum, q is the charge of an electron, m_e is the electron rest mass, γ is the Lorentz factor, and $\boldsymbol{\delta E}$ and $\boldsymbol{\delta B}$ are the electric and magnetic field perturbations that satisfy the dispersion relation of the parallel propagating whistler mode wave. When electrons interact with the waves, the equation of motion is numerically solved with the time step δt during Δt, where δt is chosen to resolve the gyromotion and Δt is the time step chosen to solve the adiabatic guiding center motion. After calculation of the momentum change in Δt, the first adiabatic invariant of the electron at $t + \Delta t$ is calculated using the background magnetic field intensity at the electron position. Simultaneously with the scattering process, the electron guiding center position is advanced, in keeping with the first and second adiabatic invariants. GEMSIS-RBW has previously been applied for simulating PsA (Miyoshi et al., 2015a; b), relativistic electron microbursts (Saito et al., 2012), and relativistic electron acceleration (Saito et al., 2016).

[8]
For the perturbation components, which are the same as that reported in Miyoshi et al. (2015a), LBC are included in the model as **Figure 2 (a)**. The minimum frequency and the maximum frequencies are 1.3 kHz (0.2 fceq, where fceq is the electron cyclotron frequency at the magnetic equator) and 2.5 kHz (0.4 fceq), respectively. The LBC bursts appear every 3 s and three rising tone elements are embedded in each burst. The repeat frequency of the rising tone elements is 3 Hz, which is a typical modulation frequency of the internal modulations of PsA (Royrvik and Davis, 1978; Miyoshi et al., 2015a). The propagation latitudes of the chorus waves are essential parameters that control the maximum energy of the resonant electrons (Miyoshi et al., 2010; 2015b; Saito et al., 2012). Considering the average propagation latitude of chorus waves from the Cluster observations (Santolik et al., 2014), we assume that LBC can propagate to 30° magnetic latitudes along the field line.

[9]
To evaluate the flux from the test particle, we utilized the simple energy spectrum of trapped electrons in the equatorial plane defined as

$$j = j_0 \exp(-E / E_0),$$

where j is the differential electron flux, j_0 is the differential flux at the characteristic energy E_0, and E is the electron energy. In this study, j_0 is 10^7/cm^2 s str keV at E_0 = 200 keV. The ambient electron density n is assumed to be a constant ($n = 3$/cm^3) along the field line of L-shell of 5.2. The wave amplitude of LBC is 100 pT.

3 Results

[10]
Figure 2 (a) shows the frequency-time diagram at the magnetic equator. As we have mentioned, we put two bursts of LBC that include three rising tone elements. **Figure 2 (b)** is the full energy spectrum of the precipitating electrons at the ionospheric altitudes. Two precipitations are clearly observed in association with the two LBC bursts. Firstly, we observed the faint precipitations that show the expected energy spectrum, where the low energy electrons arrive after the high

energy electrons at t=100 ms. These electrons are not resonant with the chorus waves and are scattered into the loss cone without the resonance. Subsequently, we observed precipitations with large flux. Electrons of energy of ~30 keV are observed at t=500 ms, and subsequently higher and lower energy electrons arrive.

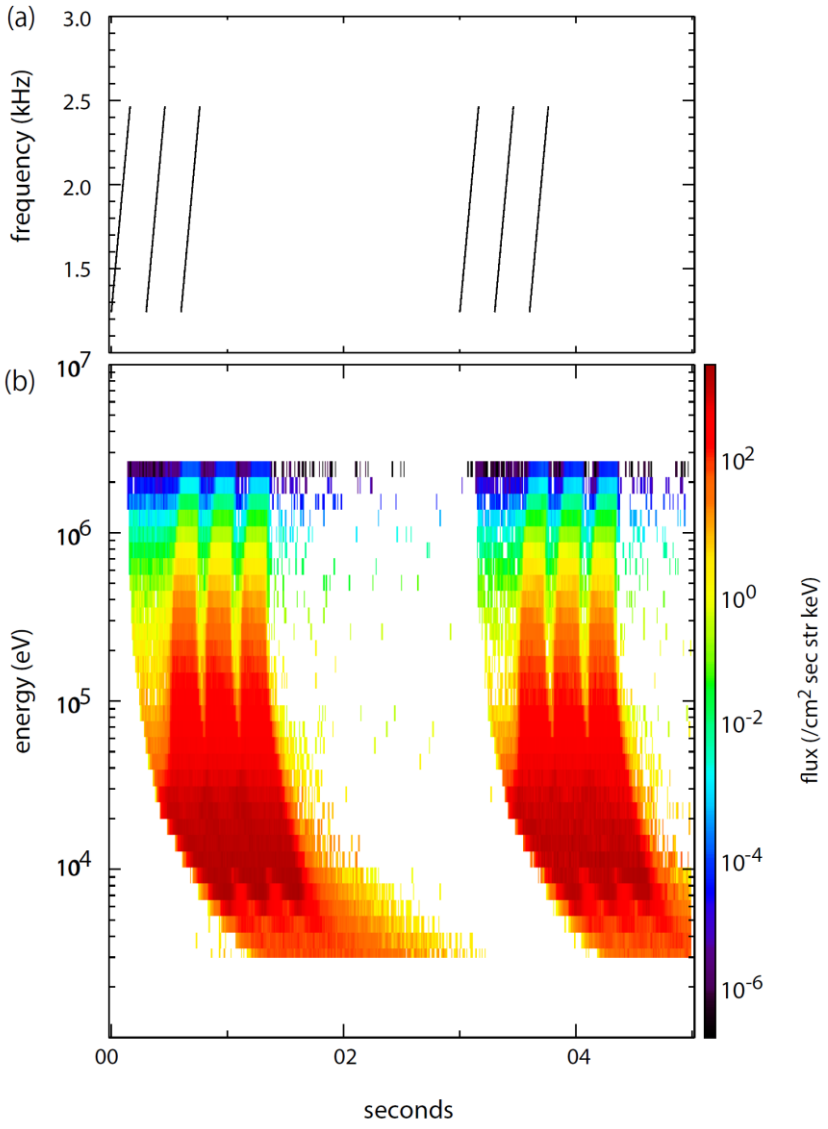

Figure 2. (a) Frequency-time diagram at the magnetic equator. There are two lower-band chorus bursts that include three rising tones in 5 seconds. (b) Variation of the precipitating electron flux with time at an altitude of 100 km calculated by the GEMSIS-RBW simulation. The color indicates the precipitating electron flux

[11]
Figure 3 shows variations of the flux of the precipitating electrons at different energies with respect to time. As another characteristic of the precipitating electrons, individual burst elements are clearly found at more than 100 keV. These burst element signatures with sharp enhancements and short durations are similar to the microbursts of sub-relativistic/relativistic electrons. In this simulation, each rising tone element causes each precipitation burst element. Two burst trains that include three individual burst element precipitations are also seen. Since LBC bursts are assumed to appear every three seconds in this simulation as shown in **Figure 2(a)**, burst trains also appear in the same time scale as the chorus bursts.

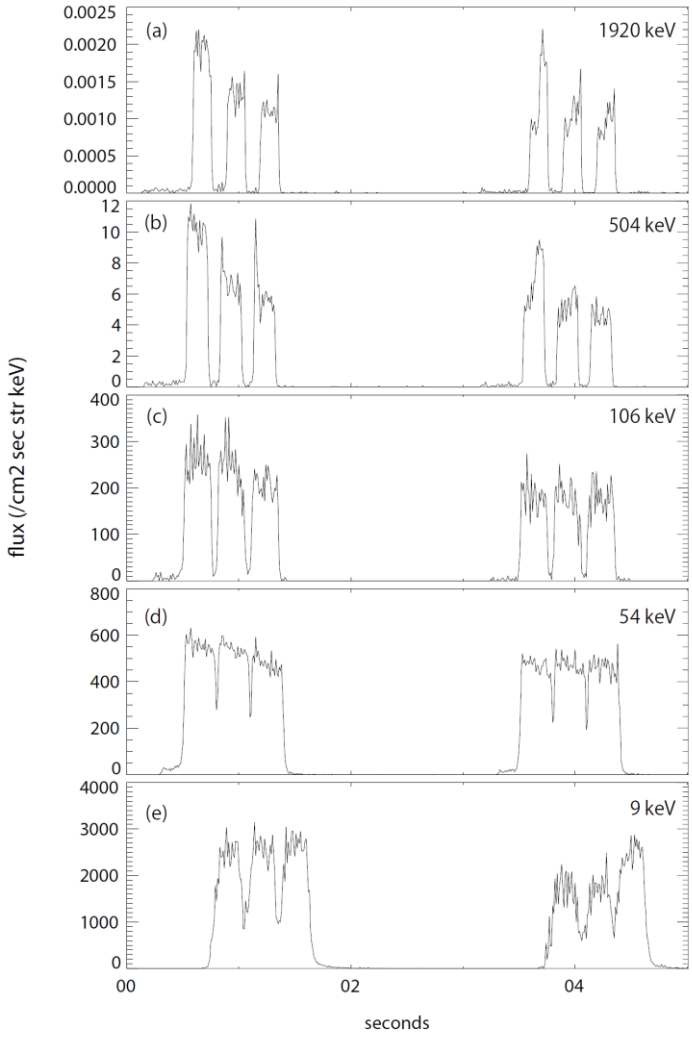

Figure 3. Temporal variation of the precipitating electrons at selected energies.

[12]
Electrons with energies less than 100 keV do not show clearly separated burst elements because the velocity dispersion leads to broader distributions. As discussed in Miyoshi et al.[2010], different frequencies of the rising tone cause resonance of ~keV - tens keV electrons at different

latitudes, which occur at different timings, so precipitation at the lower energy range is continuously observed without a significant gap during the time interval of chorus bursts. Significant electron flux enhancements are seen every 3 s, and flux modulations with 3 Hz are seen in each burst, which correspond to the main modulations and internal modulations of PsA electrons (Miyoshi et al., 2015a), respectively.

[13]
The results show that the precipitations of PsA electrons with energies of tens of keV and sub-relativistic/relativistic electrons are the same precipitation element. It is clearly shown that microbursts of sub-relativistic/relativistic electrons are the high-energy tail of PsA electron precipitation.

4 Summary and Discussions

[14]
In this study, we have conducted computer simulations for chorus wave-particle interactions to understand the energy spectrum variations of precipitating electrons associated with PsA. We confirm the hypothesis that chorus waves cause wide energy electron precipitations with energies ranging from a few keV (PsA) to more than several MeV (relativistic electron microbursts) simultaneously.

[15]
Time variations of precipitating electrons strongly depend on the electron energy. The main modulations and internal modulations of the PsA electrons are found to have energies from a few keV to tens of keV, which are related to the LBC frequency spectrum as shown by Miyoshi et al. (2015a). Precipitation caused by each rising tone element of LBC have a significant duration due to the velocity dispersion, and therefore, the precipitating electron flux has internal modulations within the main modulation at tens of keV. At the sub-relativistic/relativistic energy range, the duration of the precipitating electrons is too short to generate the main modulation that looks the same as the PsA electrons (Rosenberg et al., 1981, Lazutin, 1986); instead a series of individual burst precipitations make microburst trains. These variations are consistent with typical PsA and microburst variations. Note that multi-interactions between relativistic/sub-relativistic electrons and LBC causes a precipitation pattern like the main modulations, which have been observed (e.g., Nakamura et al., 1995).

[16]
The higher energy electrons resonate with the chorus waves at higher latitudes (Horne and Thorne, 2003; Miyoshi et al., 2015b). According to the model proposed by Miyoshi et al. (2010; 2015b), the higher energy electrons travel the longer distance from the modulation region at the high latitudes to the ionospheric altitudes at the opposite hemisphere, resulting in the arrival of the higher energy electrons after the middle energy electrons. In contrast, electrons of the order of 10 keV arrive later because of the natural time-of-flight effects. Therefore, an energy dispersion can be found, i.e, following arrival of tens keV electrons, lower energy electrons and sub-relativistic/relativistic electron precipitations are found (Miyoshi et al., 2010; Saito et al., 2012).

[17]

Figure 4 shows a schematic diagram on the relationship between the temporal variations of chorus waves at the magnetic equator, PsA and relativistic electron microbursts. Rising tone elements of LBC cause individual burst precipitations that are observed as microbursts of relativistic electrons and internal modulations of PsA electrons. The LBC bursts, that are a bundle of rising tone elements, correspond to the microburst train of relativistic electrons and the main modulations of PsA.

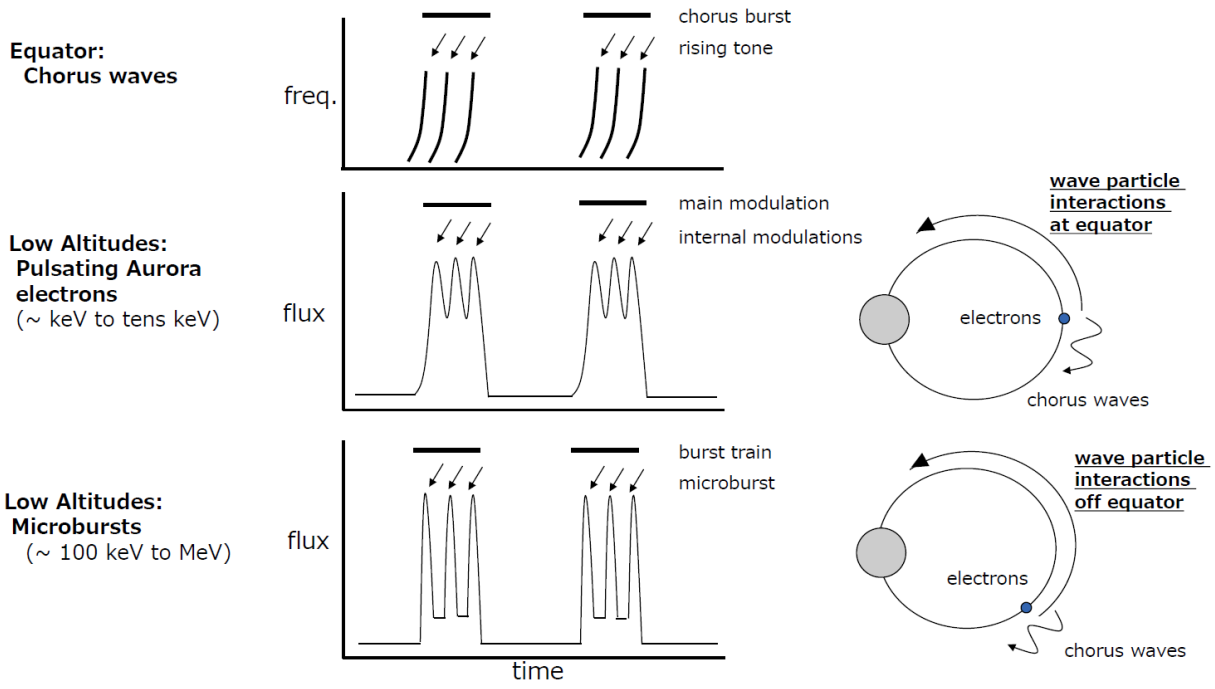

Figure 4. Schematic shows a possible connection between the temporal variations of chorus waves, PsA electrons, and relativistic electron microbursts.

[18]

Differences between relativistic electron microbursts and PsA electrons are caused by the resonance energy, which depend on the wave frequency and the magnetic latitudes. According to the resonance condition (e.g., Miyoshi et al., 2015b), the resonance with PsA electrons occurs around the magnetic equator, while the resonance with MeV electrons occurs at the higher magnetic latitudes. The maximum energy of the high-energy tail of PsA, i.e., relativistic electron microbursts, is determined by the minimum frequency of LBC and the maximum propagation latitudes of LBC. The minimum energy of precipitating electrons, i.e., the PsA electron, is determined by the maximum frequency of LBC and the generation latitudes of LBC that is typically considered to be around the magnetic equator. In this simulation, the maximum energy of the high-energy tail of PsA is 3 MeV, which is determined by the maximum propagation latitudes of LBC and the minimum frequency of LBC.

[19]

If LBC can propagate to the higher magnetic latitude, the energy of sub-relativistic/relativistic electron microbursts becomes higher, and both PsA and sub-relativistic/relativistic electron microbursts are simultaneously observed. On the other hand, if the chorus waves do not propagate to the higher magnetic latitudes, the maximum energy of precipitating electrons becomes small, and it is expected that only tens keV electron precipitations are found. Therefore, PsA does not always occur concurrently with sub-relativistic/relativistic electron microbursts.

[20]
Saito et al.[2012] has shown modulation of higher frequencies than the repetition periods of the LBC elements. They have discussed that these high frequency modulations are due to the modulation of the pitch angle distribution near the loss cone edge through nonlinear scattering by LBC. In this simulation, we have found similar high frequency modulations in the all energy range as shown in **Figure 3**, and we suggest that nonlinear wave-particle interactions cause the fast modulations of PsA and relativistic/sub-relativistic microbursts.

[21]
Recently, it has been proposed that relativistic electron precipitation causes significant ionization in the middle atmosphere and the consequent depletion of the ozone layer (e.g., Turunen et al., 2016). Our study indicates that the relativistic electron microbursts caused by the pitch angle scattering of chorus waves are the sub-product of PsA electrons, so that the continuous active PsA (e.g., Jones et al., 2013) may be a proxy for relativistic electron microbursts and the subsequent localized depletion of the ozone layer.

[22]
Blum et al.[2015] examined relativistic electron precipitations by the SAMPEX satellite, and they identified different microburst precipitations of relativistic electrons with the time scale of milliseconds and precipitation bands with longer-duration (e.g., Nakamura et al., 2000). Based on different local time distributions between microbursts and precipitation bands, they suggested that chorus waves contribute to microburst of relativistic electrons in mainly post-midnight and dawn side, while electro-magnetic ion cyclotron (EMIC) waves cause precipitation bands in mainly on the pre-midnight and dusk side. MeV electron precipitation caused by EMIC waves often occurs associated with the proton aurora at the sub-auroral latitudes (Miyoshi et al., 2008), and MeV electron precipitation with tens keV proton precipitation and without tens keV electron precipitation is caused by EMIC waves. We expect that the proton aurora is a proxy of precipitation bands caused by EMIC waves, while PsA is a proxy of microbursts caused by the chorus waves.

[23]
Through this study, we demonstrate that sub-relativistic/relativistic electron microbursts are the high-energy tail of pulsating aurora electrons. This result will be confirmed by a future sounding rocket experiment that measures wide energy electron precipitations. The LAMP (Loss through Auroral Microburst Pulsations) sounding rocket experiment is being prepared to confirm this hypothesis by measuring the energy dispersion of the precipitating electrons of PsA and sub-relativistic/relativistic electron microbursts.

Acknowledgments and Data

This work is supported by JSPS KAKENHI (15H05747, 16H06286, 17H00728, 20H01955, 20H01959). The REIMEI EISA data are opened to the public from DARTS at ISAS/JAXA (https://darts.isas.jaxa.jp/stp/reimei/). The SAMPEX HILT data are available from the SAMPEX Data Center (http://www.srl.caltech.edu/sampex/DataCenter/).

References

Anderson, K. A., and D. W. Milton (1964), Balloon observations of X-rays in the auroral zone, 3, High time resolution studies, J. Geophys. Res., 69, 4457-4479, doi: 10.1029/JZ069i021p04457.

Asamura, K., D. Tsujita, H. Tanaka, Y. Saito, T. Mukai, and M. Hirahara (2003), Auroral particle instrument onboard the INDEX satellite, Adv.Space Res., 32(3), 375–378, doi:10.1016/S0273-1177(03)90275-4.

Blake, J. B., M. D. Looper, D. N. Baker, R. Nakamura, B. Klecker, and D. Hovestadt (1996), New high temporal and spatial resolution measurements by SAMPEX of the precipitation of relativistic electrons, Adv. Space Res., 18, 171–186.

Blum, L., X. Li, and M. Denton (2015), Rapid MeV electron precipitation as observed by SAMPEX/HILT during high-speed stream-driven storms, J. Geophys. Res., 120, 3783-3794, doi:10.1002/2014JA020633.

Blum, L., and A. W. Breneman (2020), Observations of radiation belt losses due to cyclotron wave-particle interactions, in The Dynamic Loss of Earth's Radiation Belts, Elsevier, doi:10.1016/B978-0-12-813371-2.0003-2.

Cook, W. R. et al.(1993), PET a proton/electron telescope for studies of magnetospheric, solar, and galactic particles," in *IEEE Transactions on Geoscience and Remote Sensing*, vol. 31, no. 3, pp. 565-571, May 1993, doi: 10.1109/36.225523.

Breneman, A. W., et al. (2017). Observations directly linking relativistic electron microbursts to whistler mode chorus: Van Allen Probes and FIREBIRD II, Geophys. Res. Lett., 44, 11,265–11,272. https://doi.org/10.1002/2017GL075001

Horne, R. B., and R. M. Thorne (2003), Relativistic electron acceleration and precipitation during resonant interactions with whistler-mode chorus, Geophys. Res. Lett., 30(10), 1527, doi:10.1029/2003GL016973.

Hosokawa, K., Y. Miyoshi, M. Ozaki, S.-I. Oyama, Y. Ogawa, S. Kurita, Y. Kasahara, Y. Kasaba, S. Yagitani, S. Matsuda, F. Tsuchiya, A. Kumamoto, R. Kataoka, K. Shiokawa, T. Raita, E. Turunen, T. Takashima, I. Shinoara and R. Fujii (2020), Multiple time-scale beats in aurora: precise orchestration via magnetospehric chorus waves, Scientific Reports, 10, 3380, doi:10.1038/s41598-020-59642, 8.

Imhof,W. L., H. D. Voss, J. Mobilia, D. W. Datlowe, E. E. Gaines, and J. P. McGlennon (1992), Relativistic electron microbursts, J. Geophys. Res., 97,13,829–13,837, doi:10.1029/92JA01138.

Jaynes, A. N., M. R. Lessard, J. V. Rodriguez, E. Donovan, T. M. Loto'anu, and K. Rychert (2013), Pulsating auroral electron flux modulations in the equatorial magnetosphere, J. Geophys. Res., 121, doi:10.1002/2016JA022921.

Jones, S., M. Lessard, P. Fernandes, D. Lummerzheim, J. Semeter, C. Heinselman et al.(2009), PFISR and ROPA observations of pulsating aurora, J. Atm. Solar-Terr. Phys., 71, 708-716, doi:10.1016/j.jastp.2008.10.004.

Jones, S. L., M. R. Lessard, K. Rychert, E. Spanswick, E. Donovan, and A. N. Jaynes (2013), Persistent, widespread pulsating aurora: A case study, J. Geophys. Res., 118, 2998-3006.

Kasahara, S., Y. Miyoshi, S. Yokota, T. Mitani, Y. Kasahara, S. Matsuda, A. Kumamoto, A. Matsuoka, Y. Kazama, H.U. Frey, V. Angelopoulos, S. Kurita, K. Keika, K. Seki, and I. Shinohara (2018), Pulsating aurora from electron scattering by chorus waves, Nature, 554, 337-340, doi:10.1038/nature25505.

Klecker. B. et al.(1993), HILT: a heavy ion large area proportional counter telescope for solar and anomalous cosmic rays, IEEE Transactions on Geoscience and Remote Sensing, 31, 542-548, doi: 10.1109/36.225520.

Kurita, S., A. Kadokura, Y. Miyoshi, A. Morioka, Y. Sato, and H. Misawa (2015), Relativistic electron precipitations in association with diffuse aurora: Conjugate observation of SAMPEX and the all sky TV camera at Syowa Station, Geophys. Res. Lett., 42, 4702-4208, doi:10.1002/2015GL064564.

Lazutin, L. L. (1986), X-ray emission of auroral electrons and magnetospheric dynamics, Springer-Verlag, Berlin, 1986.

Lessard, M. (2012), A review of pulsating aurora, in Auroral Phenomenology and Magnetospheric Processes: Earth and Other Planets, Geophys. Monogr. Ser., edited by A. Keiling et al., pp. 55–68, AGU, Washington, D. C.

Mason, G. M., et al.(1993), LEICA: a low energy ion composition analyzer for the study of solar and magnetospheric heavy ions, IEEE Transactions on Geoscience and Remote Sensing, 31, 3, 549-556, doi: 10.1109/36.225521.

Miyoshi, Y., K. Sakaguchi, K. Shiokawa, D. Evans, J. Albert, M. Connors, and V. Jordanova (2008), Precipitation of radiation belt electrons by EMIC waves, observed from ground and space, Geophys. Res. Lett., 35, doi:10.1029/2008GL035727.

Miyoshi, Y., Y. Katoh, T. Nishiyama, T. Sakanoi, K. Asamura, and M. Hirahara (2010), Time of flight analysis of pulsating aurora electrons, considering wave-particle interactions with propagating whistler mode waves, J. Geophys. Res., 115, A10312, doi:10.1029/2009JA015127.

Miyoshi, Y., S. Saito, K.Seki, T. Nishiyama, R. Kataoka, K. Asamura, Y. Katoh, Y. Ebihara, T. Sakanoi, M. Hirahara, S. Oyama, S. Kurita, and O. Santolik (2015a), Relation between energy spectra of pulsating aurora electrons and frequency spectra of whistler-mode chorus waves, J. Geophys. Res., 120, 7728-7736, doi:10.1002/2015JA021562

Miyoshi, Y., et al. (2015b), Energetic electron precipitation associated with pulsating aurora: EISCAT and Van Allen Probes observations, J.Geophys. Res. Space Physics, 120, 2754–2766, doi:10.1029/2014JA020690.

Miyoshi, Y., I. Shinohara et al. (2018), Geospace Exploration Project ERG, Earth Planets Space, 70:101, doi:10.1186/s40623-018-0862-0.

Nakamura, R., D. N. Bake, J. B. Blake, S. Kanekal, B. Klecker, and D. Hovesta (1995), Relativistic electron precipitation enhancements near the outeredge of the radiation belt, Geophys. Res. Lett., 22, 1129–1132, doi:10.1029/95GL00378.

Nakamura, R. et al. (2000), SAMPEX observations of precipitation bursts in the outer radiation belt, J. Geophys. Res., 105, doi:10.1029/2000JA900018.

Nishimura, Y., et al. (2010), Identifying the drive of pulsating aurora, Science, 330, 81–84.

Nishimura, Y., M. R. Lessard, Y. Katoh, Y. Miyoshi, E. Grono, N. Partamies, N. Sivadas, K. Hosokawa, M. Fukizawa, M. Samara, R. G. Michell, R. Kataoka, T. Sakanoi, D. K. Whiter, S. Oyama, Y. Ogawa, and S. Kurita (2020), Diffuse and pulsating aurora, Space Sci. Rev., 216:4, doi:10.1007/s11214-019-0629-3.

Oyama, S., A. Kero, C. J. Rodger, M. A. Clilverd, Y. Miyoshi, N. Partamies, E. Turunen, T. Raita, P. T. Verronen, and S. Saito (2017), Energetic electron precipitation and auroral morphology at the substorm recovery phase, J. Geophys. Res., 122, doi:10.1002/2016JA023484.

Ozaki, M., Y. Miyoshi, K. Hosokawa et al. (2019), Visualization of rapid electron precipitation via chorus element wave-particle interactions, Nature Comm., 257, doi:10.1038/s41467-018-07996-z.

Rosenberg, T. J., J. C. Siren, et al.(1981), Conjugacy of electron microbursts and VLF chorus, J. Geophys. Res., 86, 5819-5832.

Royrvik, O., and T. N. Davis (1977), Pulsating aurora: Local and global morphology, J. Geophys. Res., 82, 4720–4740, doi:10.1029/JA082i029p04720.

Saito, S., Y. Miyoshi, and K. Seki (2012), Relativistic electron microbursts associated with whistler chorus rising tone elements: GEMSIS-RBW simulations, J. Geophys. Res., 117, A10206, doi:10.1029/2012JA018020.

Sakanoi, T., S. Okano, Y. Obuchi, T. Kobayashi, M. Ejiri, K. Asamura, and M. Hirahara (2003), Development of the multi-spectral auroral camera onboard the INDEX satellite, Adv. Space Res., 32, 379–384, doi:10.1016/S0273-1177(3)90276-6.

Sandahl, I., L. Eliasson, and R. Lundin (1980), Rocket observations of precipitating electrons over a pulsating aurora, Geophys. Res. Lett., 7, 309–312, doi:10.1029/GL007i005p00309

Santolík, O., E. Macúšová, I. Kolmašová,N. Corni lleau-Wehrlin, and Y. de Conchy(2014), Propagation of lower-band whistler-mode waves in the outer VanAllen belt: Systematic analysis of11 years of multi-component data from the Cluster spacecraft, Geophys. Res.Lett., 41, 2729–2737, doi:10.1002/2014GL059815

Shumko, M. et al.(2018), Microburst scale size derived from multiple bounces of a microburst simultaneously observed with the Firebird-II Cubesats, Geophys. Res. Lett., 45, doi:10.1029/2018GL078925.

Shumko, M., et al. (2020). Electron microburst size distribution derived with AeroCube-6. J. Geophys. Res., 125, e2019JA027651. https://doi.org/10.1029/2019JA027651

Turunen, E., A. Kero, P. T. Verronen, Y. Miyoshi, S.-I. Oyama, and S. Saito (2016), Mesospheric ozone destruction by high-energy electron precipitation associated with pulsating aurora, J. Geophys. Res. Atmos., 121, doi:10.1002/2016JD025015.

Tsurutani, B. T., G. S. Lakhina, and O. P. Verkhoglyadova (2013), Energetic electron (>10 keV) microburst precipitation, ~5–15 s X-ray pulsations, chorus, and wave-particle interactions: A review, J. Geophys. Res. Space Physics, 118, 2296–2312, doi:10.1002/jgra.50264.

Figure 1. Variation of the precipitating electron flux with respect to time at an altitude of ~100 km. (a) Typical variations of the precipitating electrons associated with the pulsating aurora measured by Reimei. The corresponding energy is 8.7 keV. (b) Typical variations of precipitating electrons of relativistic microbursts (>1 MeV) measured by SAMPEX.

Figure 2. (a) Frequency-time diagram at the magnetic equator. There are two lower-band chorus bursts that include three rising tones in 5 seconds. (b) Variation of the precipitating electron flux with time at an altitude of 100 km calculated by the GEMSIS-RBW simulation. The color indicates the energy of the precipitating electron flux

Figure 3. Temporal variation of the precipitating electrons at selected energies.

Figure 4. Schematic shows a possible connection between the temporal variations of chorus waves, PsA electrons, and relativistic electron microbursts.

Figure.

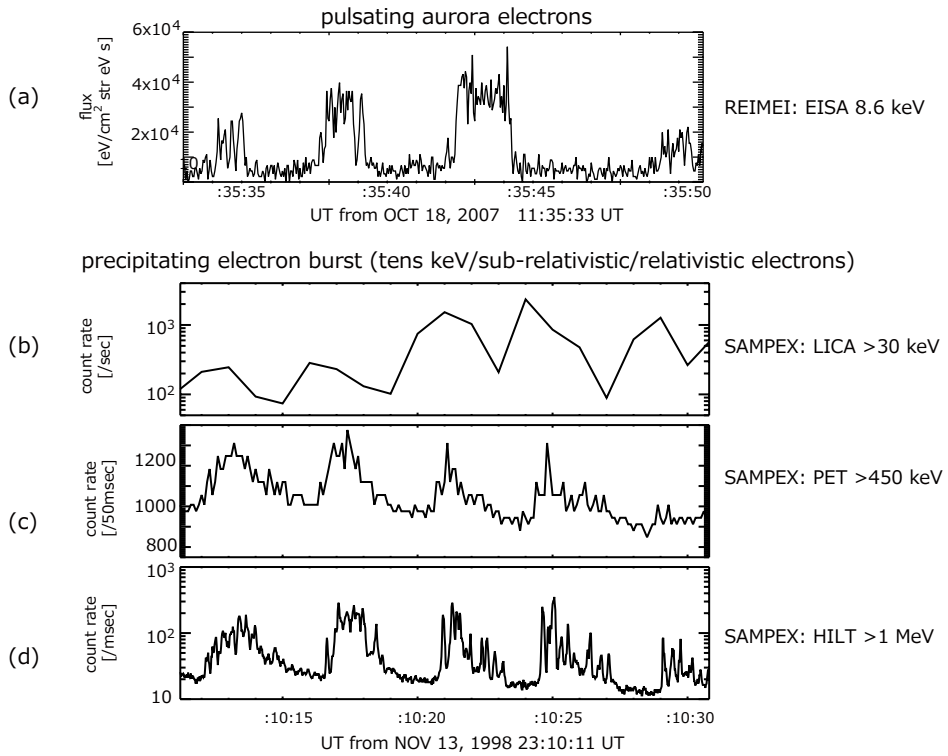
pulsating aurora electrons
(a)
6x10^4
4x10^4
2x10^4
flux
[eV/cm^2 str eV s]
:35:35
:35:40
:35:45
:35:50
UT from OCT 18, 2007 11:35:33 UT
REIMEI: EISA 8.6 keV
precipitating electron burst (tens keV/sub-relativistic/relativistic electrons)
(b)
count rate
[/sec]
10^3
10^2
SAMPEX: LICA >30 keV
(c)
count rate
[/50msec]
1200
1000
800
SAMPEX: PET >450 keV
(d)
count rate
[/msec]
10^3
10^2
10
:10:15
:10:20
:10:25
:10:30
UT from NOV 13, 1998 23:10:11 UT
SAMPEX: HILT >1 MeV

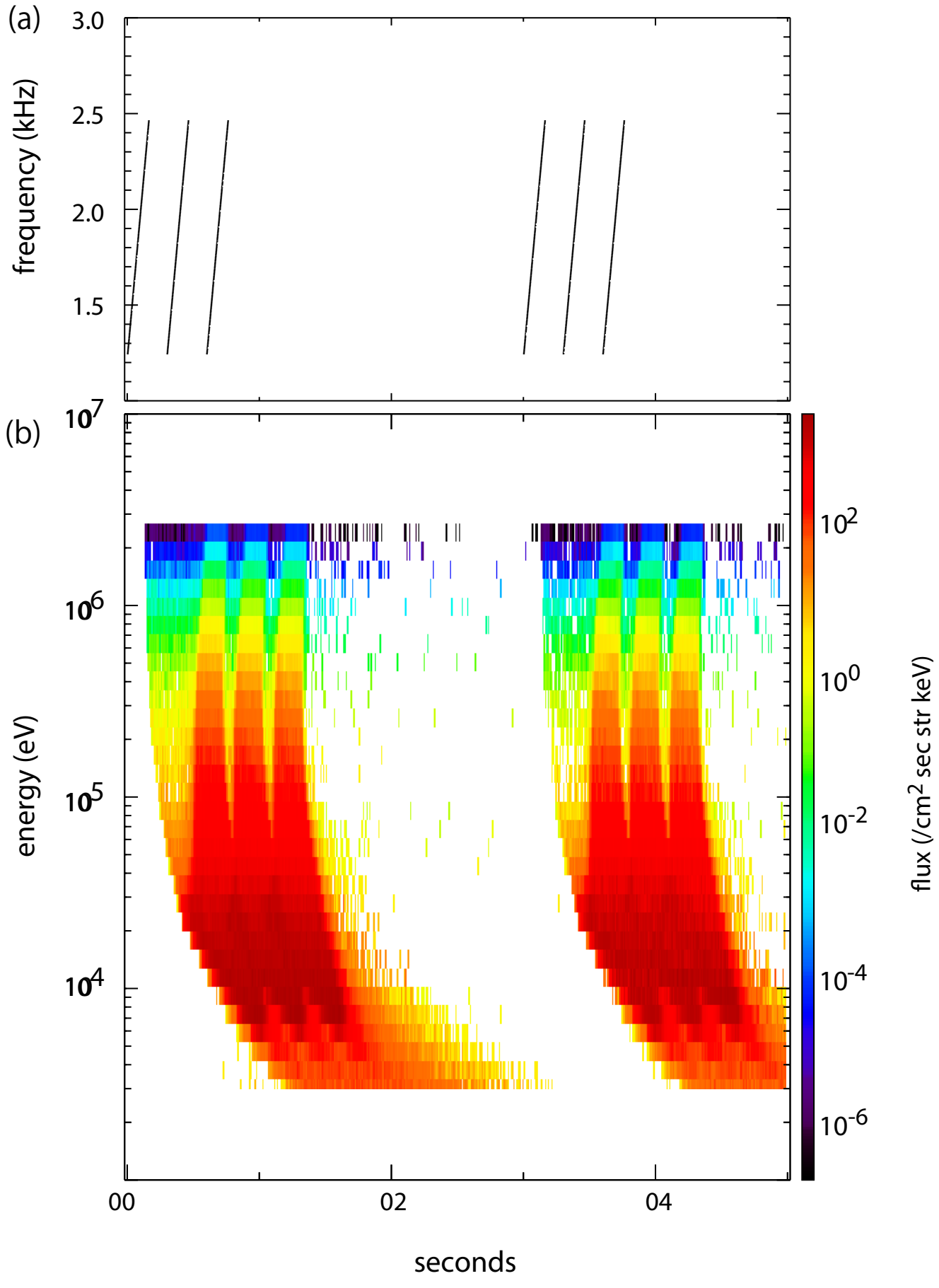
(a)
3.0
2.5
2.0
1.5
frequency (kHz)
(b)
10^7
10^6
10^5
10^4
energy (eV)
00
02
04
seconds
10^2
10^0
10^{-2}
10^{-4}
10^{-6}
flux (/cm^2 sec str keV)

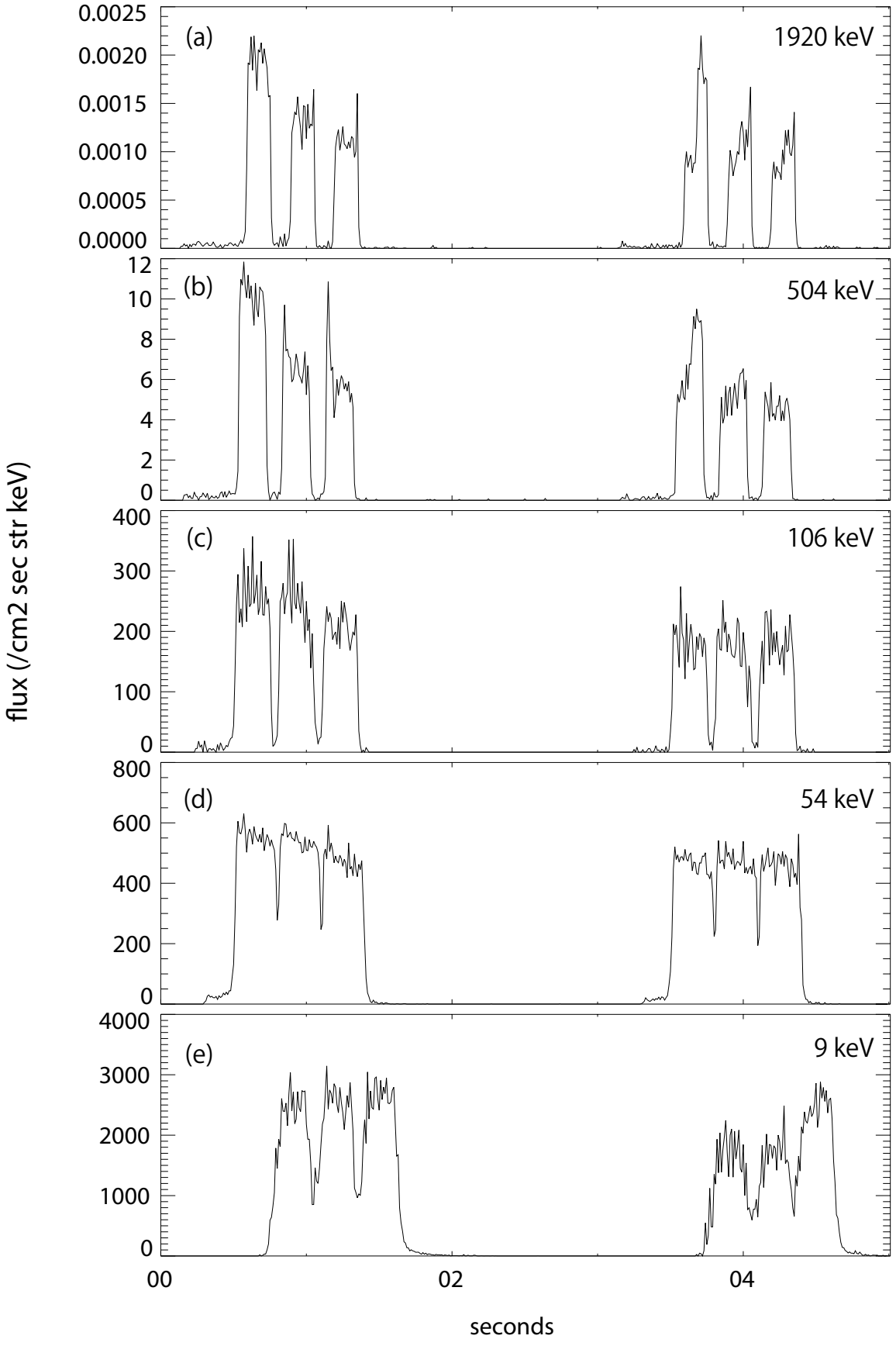
(a)
1920 keV
0.0025
0.0020
0.0015
0.0010
0.0005
0.0000
(b)
504 keV
12
10
8
6
4
2
0
(c)
106 keV
400
300
200
100
0
(d)
54 keV
800
600
400
200
0
(e)
9 keV
4000
3000
2000
1000
0
00
02
04
seconds
flux (/cm2 sec str keV)

Equator:
Chorus waves

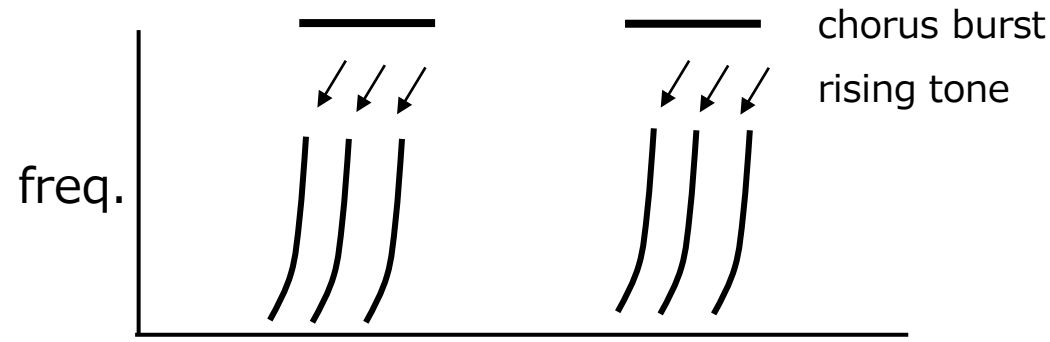

Low Altitudes:
Pulsating Aurora electrons
(~ keV to tens keV)

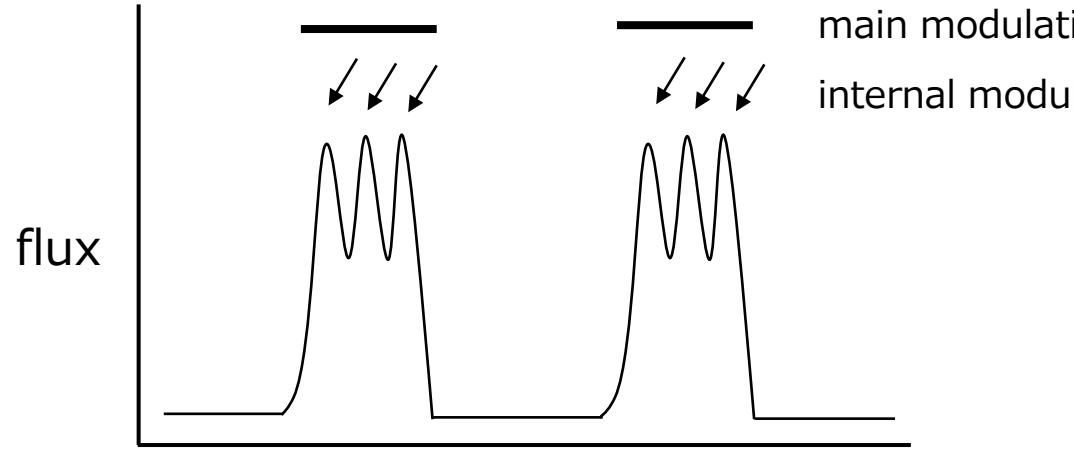

Low Altitudes:
Microbursts
(~ 100 keV to MeV)

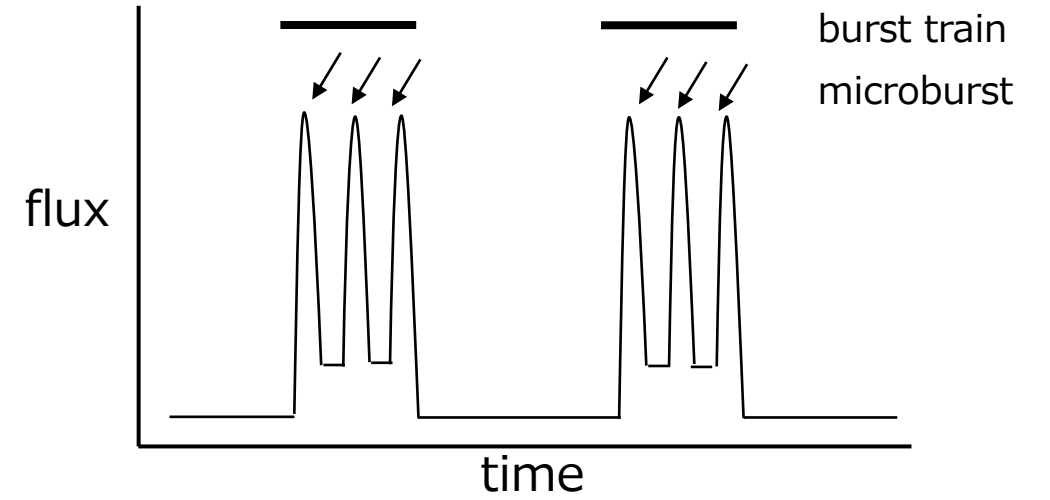

wave particle interactions at equator

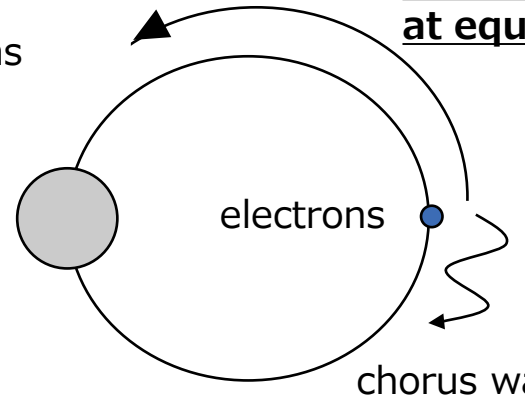

wave particle interactions off equator